

Panel Zone Deformation Capacity as Affected by Weld Fracture at Column Kinking Location

DONG-WON KIM, COLIN BLANEY and CHIA-MING UANG

ABSTRACT

Three full-scale specimens were tested to evaluate the cyclic performance of rehabilitated pre-Northridge steel beam-to-column moment connections. A Kaiser bolted bracket (KBB) was used on the beam bottom flange for all specimens, but different rehabilitation schemes (another KBB, a notch-tough beam flange replacement weld, or a double-tee welded bracket) were used to strengthen the top flange. All specimens were able to sustain an interstory drift angle of 0.04 radian, with large inelastic deformations in the panel zone. Two specimens experienced fracture at the replacement complete-joint-penetration (CJP) welds, mainly due to the large shear deformation in the panel zone. Because it may not be economically feasible to mitigate weak panel zones in seismic rehabilitation, an analytical model was developed to predict the panel zone deformation capacity and the associated strength. In this model, it was postulated that the ultimate panel zone deformation capacity corresponded to that when each column flange was fully yielded and excessive kinking would cause fracture of the beam flange CJP welds. This postulation was verified by the test data of two specimens that experienced weld fracture due to excessive panel zone deformation. It was shown that the deformation capacity is a function of d_b/t_{cf} (beam depth-to-column flange thickness ratio). The effect of column axial load was also studied.

Keywords: special moment frame, moment connection, panel zone, shear deformation, Kaiser bolted bracket, rehabilitation.

INTRODUCTION

The Kaiser bolted bracket (KBB) moment connection is a proprietary connection prequalified by AISC 358-10 (AISC, 2010a) for applications in seismic regions. In a KBB moment connection, a cast high-strength steel bracket is fastened to each beam flange and bolted to the column flange; a pair of brackets is placed symmetrically on both the top and bottom flanges of the beam. The bracket attachment to the beam flange can be either welded (W-series brackets) or bolted (B-series brackets). Figure 1 shows one example of a bolted KBB connection, and Figure 2 shows one of the two bolted brackets prequalified by AISC. The prequalification is mainly based on full-scale tests (Kasai, Hogdon and Bleiman, 1998, Gross et al., 1999, Newell and Uang 2006); see Adan and Gibb (2009) for a summary of the development of this connection.

Note that AISC 358-10 is intended for new construction, not seismic rehabilitation. When bolted KBB connections

are used, one major advantage is to eliminate field welding. This is desirable, especially for seismic rehabilitation of existing steel moment frame buildings. The bracket configuration is proportioned to develop the probable maximum moment strength of the connected beam. According to AISC 358-10, yielding and plastic hinge formation are intended to occur primarily in the beam at the end of the bracket away from the column face. Limited yielding in the column panel zone may occur, and the panel zone shear strength per AISC 341-10 (AISC, 2010b) needs to be satisfied. The beam size is limited to W33×130.

The KBB connections were recently proposed for the seismic rehabilitation of a pre-Northridge steel moment frame building (Blaney et al., 2010). Qualification tests were conducted for this project because of the following challenges. First, AISC 358-10 requires that the KBBs be symmetrically placed above and below the beam. For seismic rehabilitation, it is not architecturally desirable to place a KBB above the beam because it may extrude beyond the floor slab. It has been shown, however, that the bottom-only bracket configuration cannot prevent fracture of the beam top flange complete-joint-penetration (CJP) groove weld in a pre-Northridge moment connection (Gross et al., 1999). Second, the beam flanges are not welded to the column flange in the AISC prequalified KBB moment connections, while this is not the case for the rehabilitated moment connections. Such a difference may alter the force transfer mechanism in the connection. Third, both the beam size and the required KBB size (type B1.0C) exceed those permitted by AISC 358-10. Finally, because steel moment frames designed and

Dong-Won Kim, Research Assistant, Department of Structural Engineering, University of California, San Diego, La Jolla, CA. Email: dwk008@ucsd.edu

Colin Blaney, Executive Principal, ZFA Structural Engineers, San Francisco, CA, Email: colinb@zfa.com

Chia-Ming Uang, Professor, Department of Structural Engineering, University of California, San Diego, La Jolla, CA (corresponding author). Email: cmu@ucsd.edu

Table 1. Width-to-Thickness Ratios			
Member	Size	$b_f/2t_f$	h/t_w
Beam	W36×150	6.37	51.9
Column	W14×193	5.45	12.8

Note: $\lambda_{hd} = 0.30\sqrt{E/F_y} = 7.22$ for flange; $\lambda_{hd} = 2.45\sqrt{E/F_y} = 59$ for web ($P_u = 0$).

constructed prior to the 1994 Northridge earthquake could have very weak panel zones, where the demand-capacity ratio for shear yielding in the panel zone is much higher than that of flexural hinging of the connected beams, and because it is not practical to rehabilitate existing moment connections to achieve the intended performance of AISC 358-10 (i.e., beam plastic hinging with limited or no panel zone yielding), full-scale testing was needed to verify the proposed connection rehabilitation scheme with a weak panel zone.

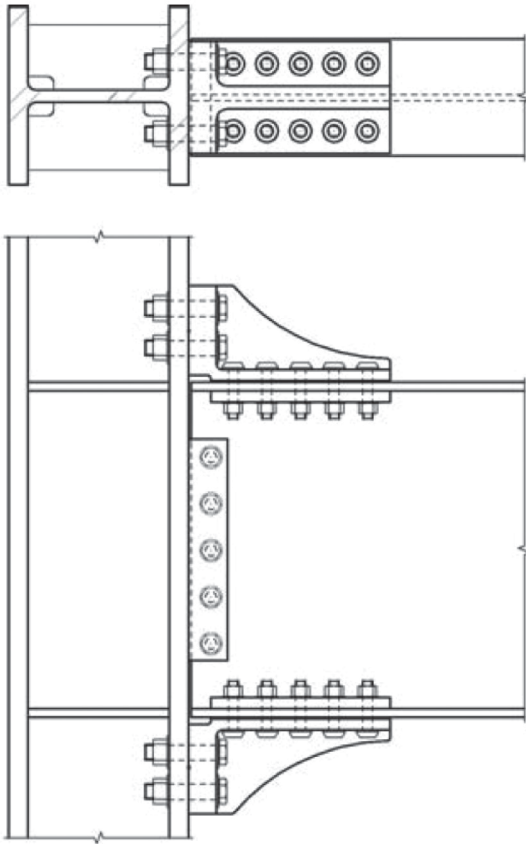


Fig. 1. KBB connection (figures reprinted from AISC, 2010a).

TEST PROGRAM

Test Specimens

A total of three nominally identical, full-scale pre-Northridge moment connections with a W36×150 beam and a W14×193 column were rehabilitated and tested. Table 1 shows that the beam and column sections satisfied the AISC 341-10 compactness requirement as highly ductile members. The pre-Northridge style, welded flange-bolted web moment connections were first fabricated and constructed following the pre-Northridge practice. Beam flange-to-column flange CJP groove welds were made with an E70T-4 electrode. Steel backing, runoff tabs, and weld dams were also used in a manner consistent with the pre-Northridge practice. Stiffeners inside the panel zone and one stiffener in the beam web were included to simulate an existing condition in the building.

For rehabilitation, runoff tabs and weld dams were removed while the steel backing remained. Then a B-series bracket (B.1.0C) was installed on the beam bottom flange of all three specimens. Table 2 summarizes the bracket details. To attach the bracket to the column and beam flanges, $1/16$ - and $1/32$ -in. oversized holes were made using a magnetic-base drill to the column and beam flanges, respectively. The high-strength bolts were fully tensioned with a calibrated hydraulic torque wrench. The treatment of the beam top flange was different for all three specimens, as described below.

For specimen 1, the same bracket was also added to strengthen the top flange (see Figure 3), a configuration required by AISC 358-10 for new construction. For

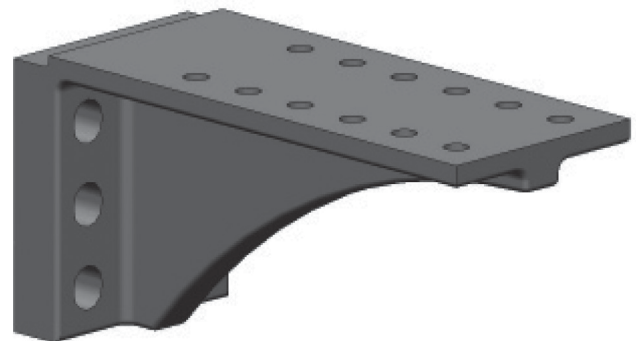
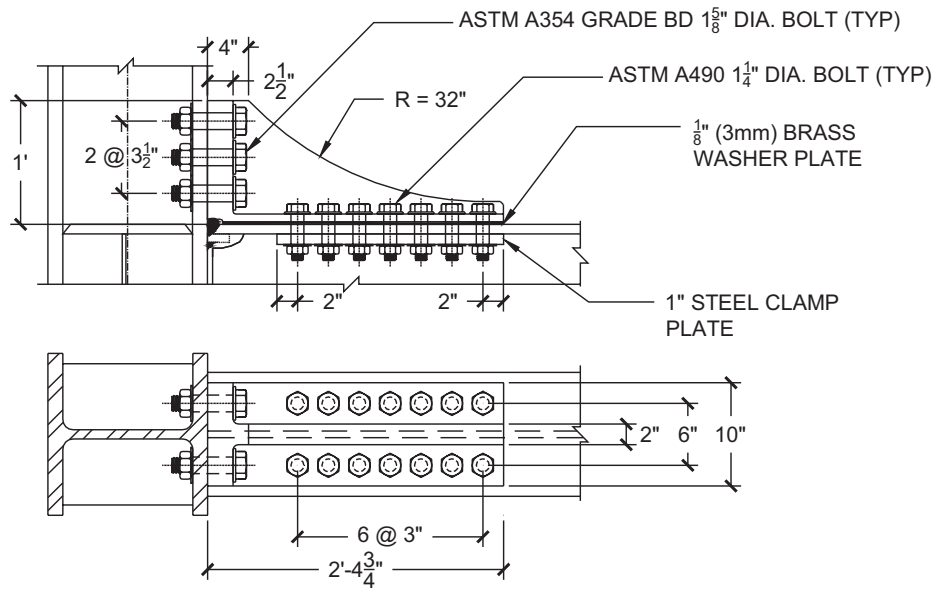
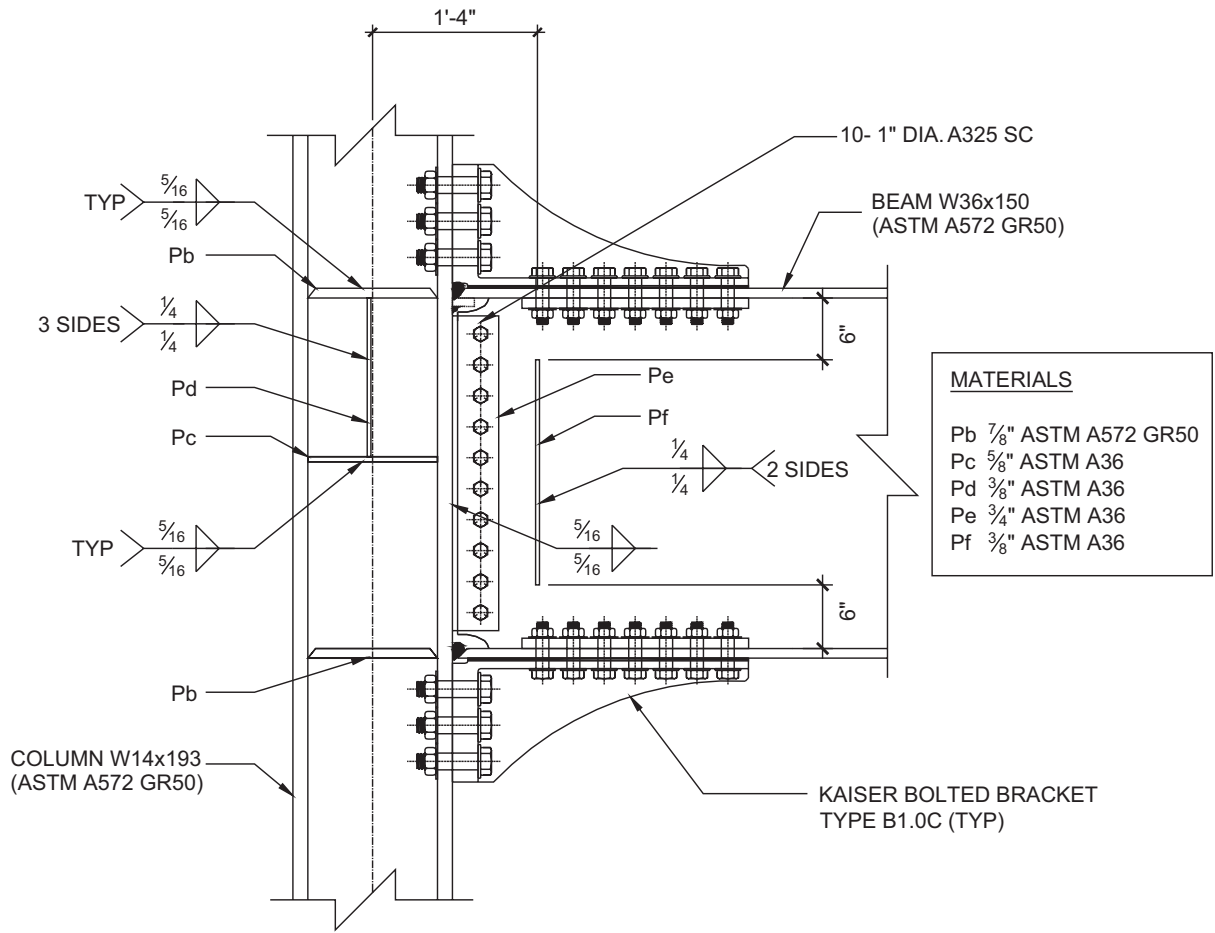


Fig. 2. KBB type B1.0 (figures reprinted from AISC, 2010a).



DETAILS OF KAISER BOLTED BRACKET (B1.0C)

Fig. 3. Specimen 1 connection details.

Table 2. Kaiser Bolted Bracket B1.0.C					
Proportions					
Bracket Length, L_{bb} (in.)	Bracket Height, h_{bb} (in.)	Bracket Width, b_{bb} (in.)	Number of Column Bolts, n_{cb}	Column Bolt Gage, g , (in.)	Column Bolt Diameter (in.)
28¾	12	10	6	6½	1⅝
Design Proportions					
Column Bolt Edge Distance, d_e (in.)	Column Bolt Pitch, p_b (in.)	Bracket Stiffener Thickness, t_s (in.)	Bracket Stiffener Radius, r_v (in.)	Number of Beam Bolts, n_{bb}	Beam Bolt Diameter (in.)
2	3½	2	32	14	1¼

See Figure 9.5 in AISC 358 for bracket parameter definition.

Table 3. Steel Member Sizes and Mechanical Properties of Specimens 1, 2 and 3			
Member	Yield Stress (ksi)	Tensile Strength (ksi)	Elongation* (%)
Beam flange (W36×150)	61.6	75.9	33
Column flange (W14×193)	62.1	80.5	31.5

*Elongation is based on a 2-in. gage length.

specimen 2, the existing beam top flange weld was gouged out and then replaced by a notch-tough CJP weld made with an E71T-8 electrode; the minimum required Charpy V-Notch impact test values were 20 ft-lb at 20 °F and 40 ft-lb at 70 °F. The steel backing remained but was reinforced with a ⅝-in. fillet weld. The existing weld access hole was not modified.

After testing of specimen 2, it was decided to not only replace the existing beam top flange CJP weld as in specimen 2 (see Figure 4), but to also strengthen the new weld with a welded double-tee bracket for specimen 3 (see Figure 5). The height of the welded bracket (5 in.) was selected to be flush with the surface of the existing concrete slab. The cross-section of the double-tee bracket was selected such that the beam top-flange stress at the column face was about 50% of the yield stress; the top-flange stress was calculated based on the elastic beam theory and a beam moment extrapolated from the probable maximum moment (M_{pr}) defined in AISC 358-10.

As noted earlier, the beam flanges were not connected to the column in the AISC 358-10 prequalified KBB connections. But CJP welds did exist in the rehabilitated moment connections. The bolted KBB brackets used had a notch to clear the existing CJP weld in the top flange and steel backing in the bottom flange.

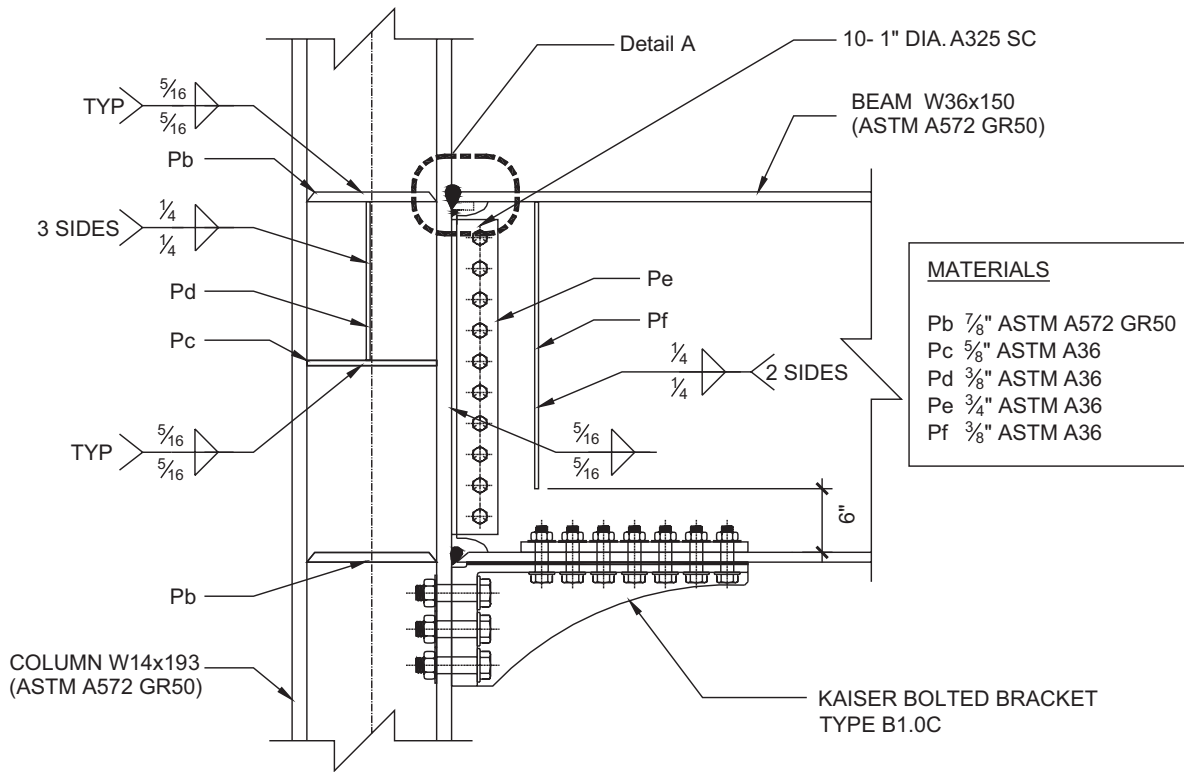
Material Properties

ASTM A572 Grade 50 steel was specified for the beams, columns, continuity plates and the double-tee bracket. A36 steel was specified for all other plates. Table 3 shows the

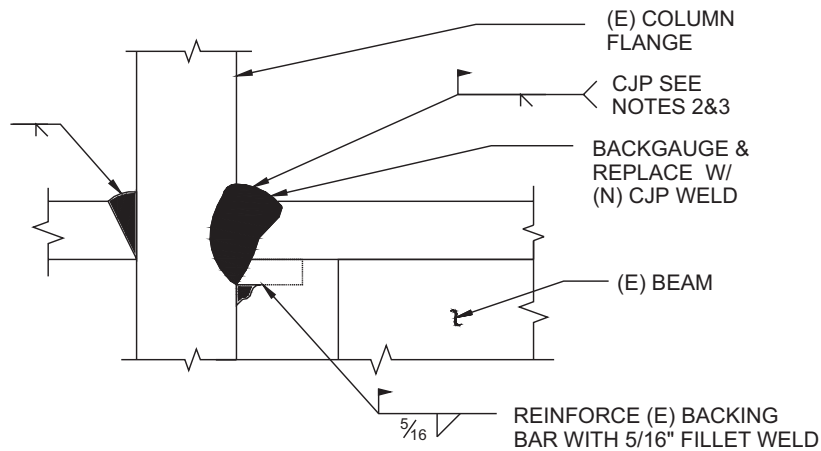
mechanical properties of the materials obtained from tensile coupon tests. The material for the KBB high-strength castings was ASTM A958 Grade SC8620, class 90/60. This material has a specified minimum yield and tensile strengths of 60 and 90 ksi, respectively. ASTM A354 Grade BD 1⅝-in.-diameter, high-strength bolts were specified for the KBB-to-column fasteners, and ASTM A490 1¼-in.-diameter, high-strength bolts were specified for the KBB-to-beam fasteners.

Design Parameters

Based on AISC 341-10 and AISC 358-10, the design parameters (column-beam moment ratio and panel zone demand-capacity ratio) were calculated as provided in Table 4. Based on both nominal yield stresses (F_y) and actual yield stresses from the tensile coupon test results, the design parameters were computed for both the existing and rehabilitated conditions. To compute the column-beam moment ratio, the beam moment (M_{pb}^*) was determined by extrapolating the expected beam plastic moment to the centerline of the column, and the column moment strength (M_{pc}^*) was calculated by extrapolating the nominal flexural strength (including haunches where used) above and below the joint to the centerline of the beam. The column-beam moment ratios, $\sum M_{pc}^* / \sum M_{pb}^*$, were greater than 1.0 in all cases, indicating a strong-column weak-beam (SC/WB) configuration. The same table also shows that the panel zone demand-capacity ratios (V_{pz}/V_n) were much larger than 1.0 for all cases, implying very weak panel zones in these rehabilitated specimens.



MATERIALS	
Pb	7/8" ASTM A572 GR50
Pc	5/8" ASTM A36
Pd	3/8" ASTM A36
Pe	3/4" ASTM A36
Pf	3/8" ASTM A36

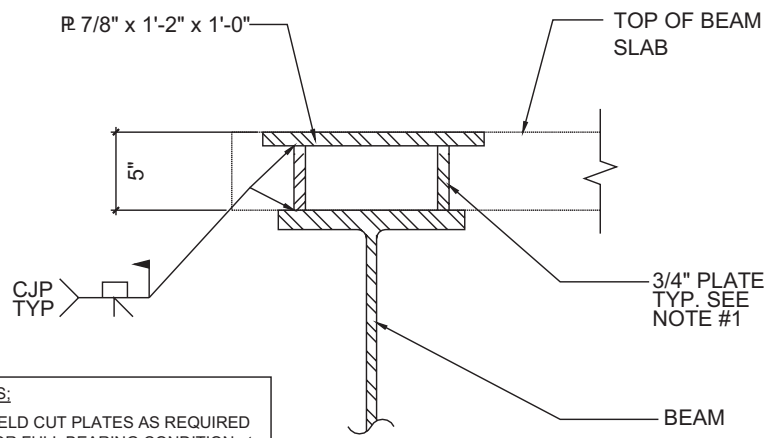
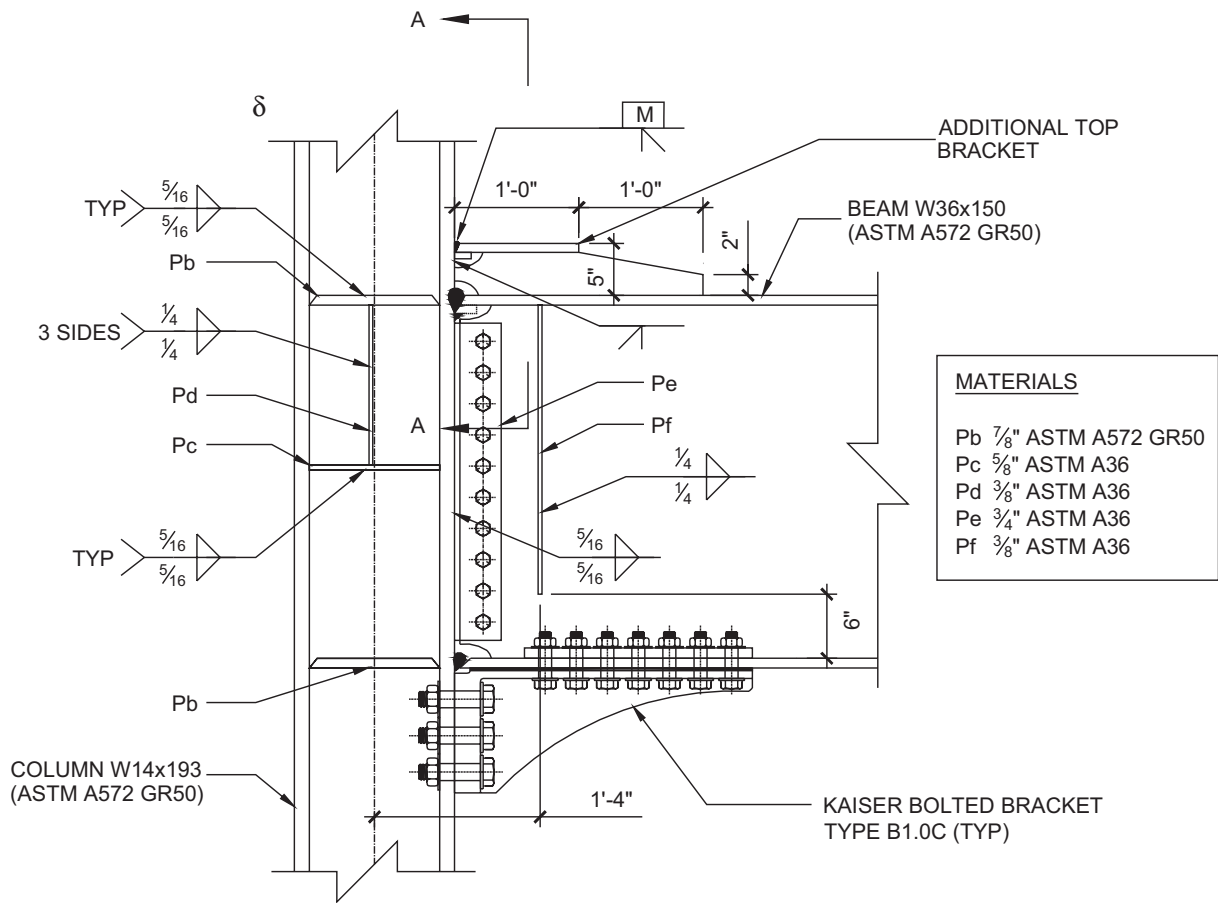


Detail A

NOTES:

1. PREPARE ORIGINAL TOP FLANGE WELD TO PRE-NORTHRIDGE CONDITION W/ CJP GROOVE WELD
2. GOUGE OUT (E) TOP FLANGE WELD & PREPARE JOINT FOR NEW WELD
3. PROVIDE (N) COMPLETE PENETRATION GROOVE WELD. (POST-NORTHRIDGE)

Fig. 4. Specimen 2 connection details.



NOTES:

1. FIELD CUT PLATES AS REQUIRED FOR FULL BEARING CONDITION at COLUMN & BEAM TRANSITION.

SECTION A - A

Fig. 5. Specimen 3 connection details.

Specimen No.	Design Parameters	Before Rehabilitation		After Rehabilitation	
		Nominal F_y	Actual F_y	Nominal F_y	Actual F_y
Specimen 1	$\sum M_{pc}^* / \sum M_{pb}^*$	1.03	1.14	1.15	1.27
	V_{pz} / V_n	1.96	1.76	1.47	1.33
Specimen 2	$\sum M_{pc}^* / \sum M_{pb}^*$	1.03	1.14	1.05	1.16
	V_{pz} / V_n	1.96	1.76	1.75	1.58
Specimen 3	$\sum M_{pc}^* / \sum M_{pb}^*$	1.03	1.14	1.09	1.20
	V_{pz} / V_n	1.96	1.76	1.53	1.38

Test Setup and Loading Sequence

Figure 6 shows the test setup. A corbel was bolted to the end of the beam and attached to two 220-kip hydraulic actuators.

With some minor modification, the loading sequence specified in Section K2 of AISC 341-10 for beam-to-column moment connection test was used. A performance-based seismic rehabilitation study established a target story drift ratio of 3.5% (Liu et al., 2009). Therefore, the AISC loading protocol was modified to include two additional cycles

at 3.5% story drift. The loading began with six cycles each at 0.375, 0.5, and 0.75% drift. The next four cycles in the loading sequence were at 1% drift, followed by two cycles each at 1.5, 2, 3, 3.5, and 4%. Beyond that, the specimens were cycled to 4.5% until failure due to the limitation of the actuator stroke. Testing was conducted in a displacement-controlled mode, and the cyclic displacement was applied at the end of the beam.

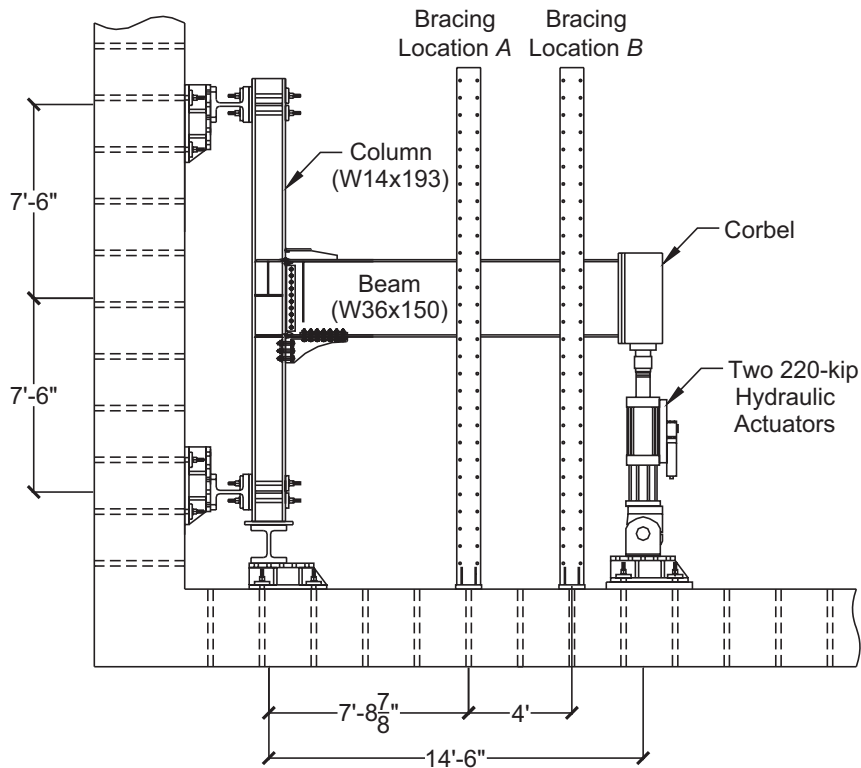


Fig. 6. Test setup (specimen 3).

TEST RESULTS

Figure 7 summarizes the damage pattern in three test specimens. The cyclic responses are presented in Figure 8. Significant shear yielding in the panel zone was observed in all three specimens. Also, the KBBs remained intact and showed no sign of yielding or damage. For specimen 1, the double KBBs forced beam plastic hinging in the form of

flange and web local buckling as well as lateral-torsional buckling near the tip of the KBBs. The testing was stopped after completing two cycles at 4.5% story drift due to significant lateral-torsional buckling of the beam. Note that one lateral brace was provided at location A in specimen 1 (see Figure 6). This corresponded to an unbraced length of 92.9 in., which was less than that (123.2 in.) permitted by AISC 341-10. Because significant lateral-torsional buckling

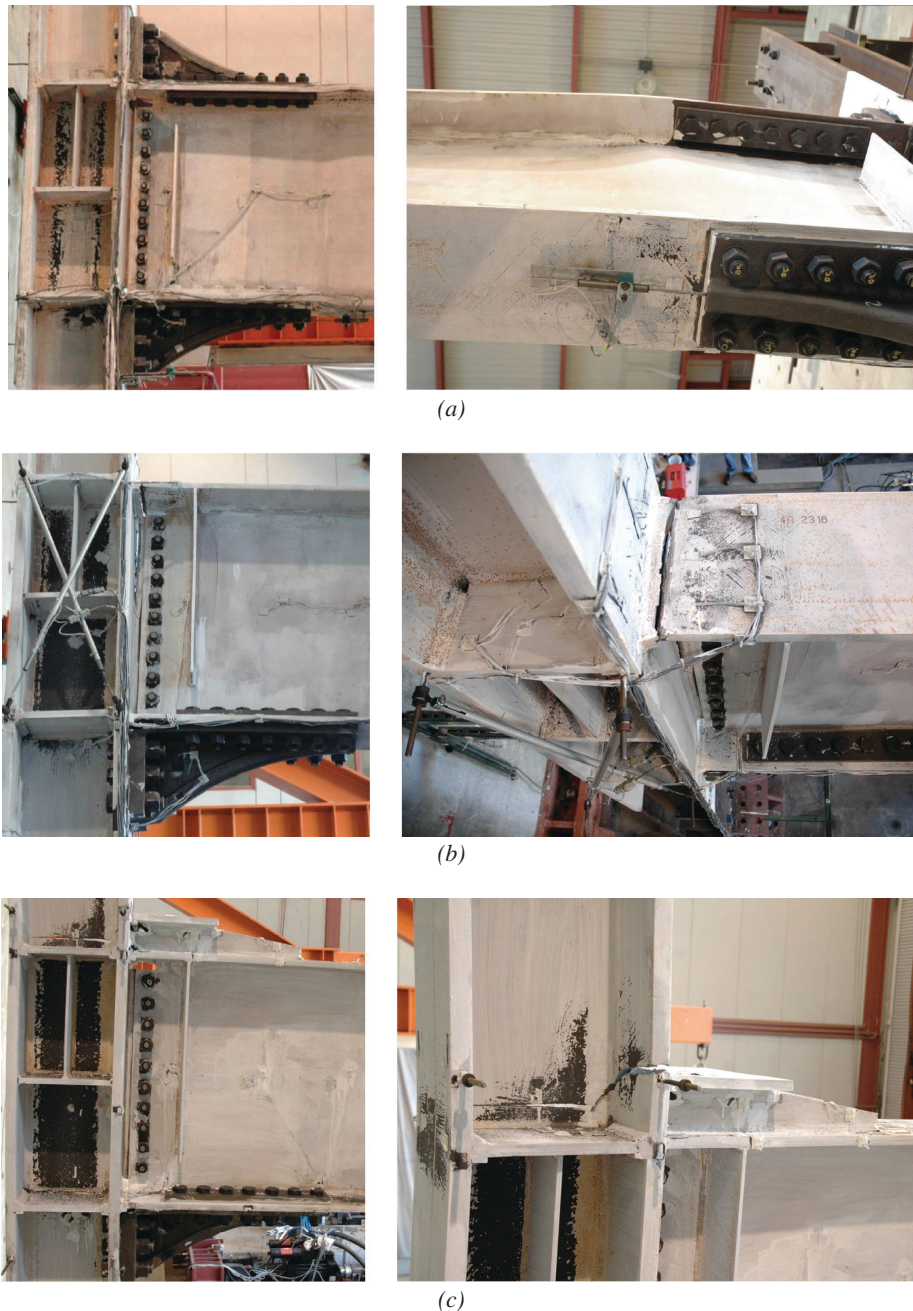


Fig. 7. Damage patterns: (a) specimen 1 panel zone yielding and beam lateral buckling; (b) specimen 2 panel zone yielding and top flange weld fracture; (c) specimen 3 panel zone yielding and top flange bracket weld fracture.

of the beam occurred in specimen 1, it was decided to add another lateral bracing at location *B* for specimens 2 and 3. The additional bracing was used to brace the top flange only to simulate the restraint provided by the concrete slab in the real building.

Specimen 2 experienced significant yielding in the panel zone, but the extent of beam plastic hinging was very limited with no sign of buckling. After completing one cycle at 4% story drift, fracture of the beam top flange at the replacement weld occurred during the second cycle (see Figure 7b).

The behavior of specimen 3 was similar to that of specimen 2—that is, inelastic action occurred mainly in the panel zone. The CJP weld connecting the horizontal plate of the double-tee bracket to the column flange started to fracture at 4% story drift. The specimen was then cycled at 4.5% story drift repeatedly until failure; see Figure 8c for the cyclic response. Brittle fracture occurred during the fifth negative cycle (see Figure 7c).

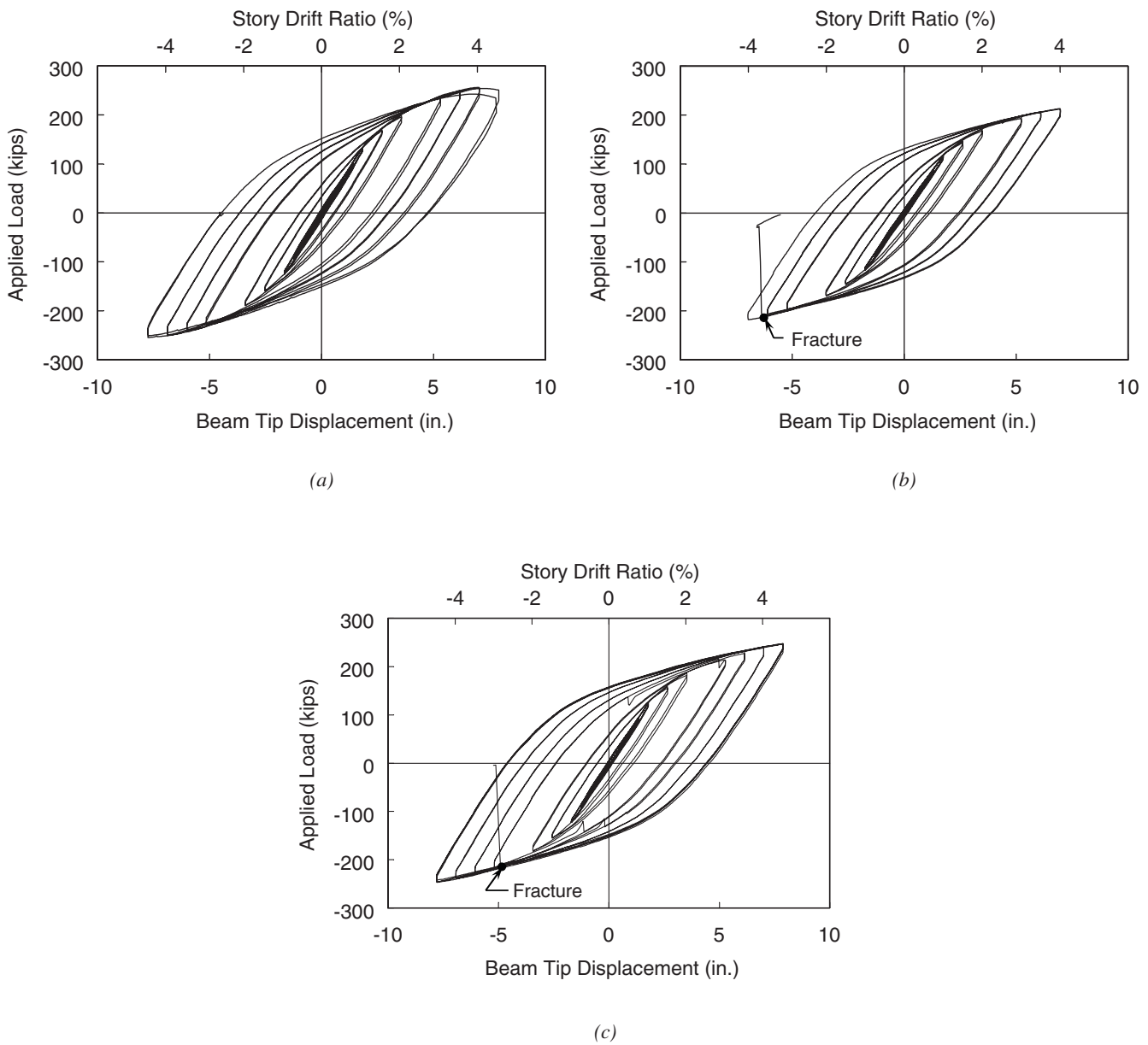


Fig. 8. Load versus beam tip displacement: (a) specimen 1; (b) specimen 2; (c) specimen 3.

PANEL ZONE BEHAVIOR

Effective Depth of Extended Panel Zone

With the addition of KBBs above and below the beam, the panel zone is extended in depth. AISC 358-10 (AISC, 2010a) defines the effective depth, d_{eff} , of the extended panel zone as the centroidal distance between column bolt groups in the upper and lower KBBs (see Figure 9a). Generalizing the AISC definition to specimens 2 and 3 with only one KBB used, the definition of d_{eff} is also shown in the figure.

The average shear deformations of the original and

extended panel zones can be computed from test data based on Equations 1 and 2:

$$\gamma_{pz} = \frac{\sqrt{a^2 + d^2}}{2ad} (\delta_1 + \delta_2) \quad (1)$$

$$\gamma_{epz} = \frac{\sqrt{a^2 + (d_{eff})^2}}{2ad_{eff}} (\delta_3 + \delta_4) \quad (2)$$

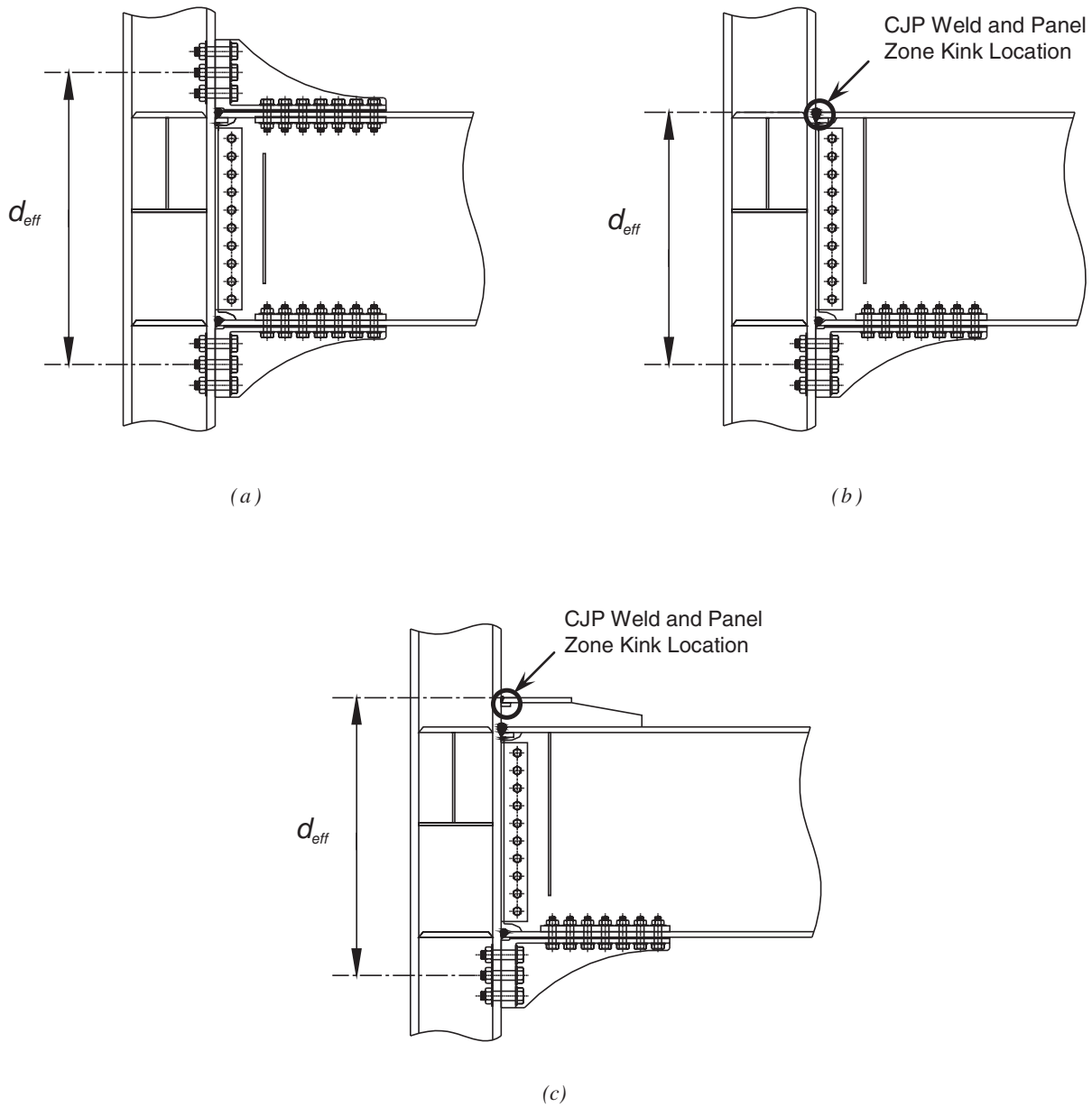


Fig. 9. Effective depth of extended panel zone: (a) specimen 1; (b) specimen 2; (c) specimen 3.

where the instrumentation for the panel zone deformations is shown in Figure 10. Figure 11 compares the shear deformations of the panel zones for all test specimens. It shows that the shear deformation was mainly concentrated in the original panel zone.

Based on a pair of diagonal measurements in the extended panel zone, the average shear deformation can be computed. The shear in the extended panel zone can also be computed by using the effective depth:

$$V = \frac{M_f}{0.95d_{eff}} - V_c \quad (3)$$

where M_f is the moment at the face of column and V_c is the shear in the column. The cyclic responses of the extended panel zones for specimens 2 and 3 are presented in Figure 12.

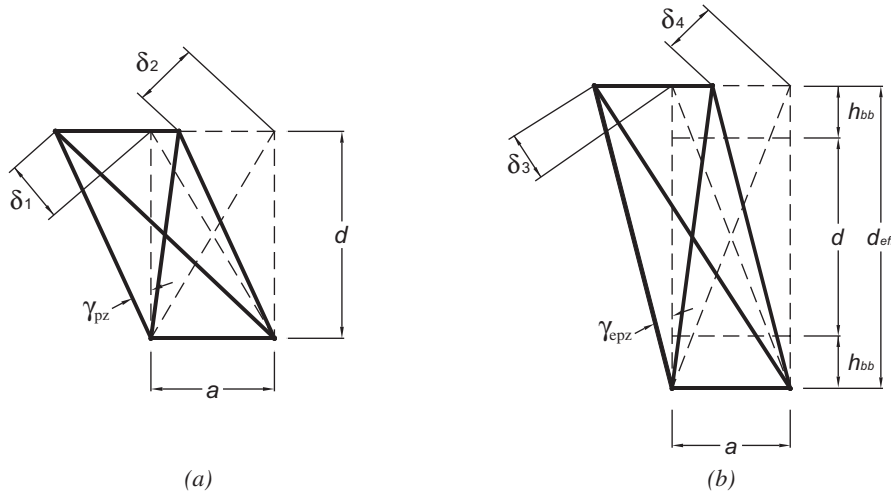


Fig. 10. Panel zone deformation measurements: (a) original panel zone before rehabilitation; (b) extended panel zone after rehabilitation (specimen 1).

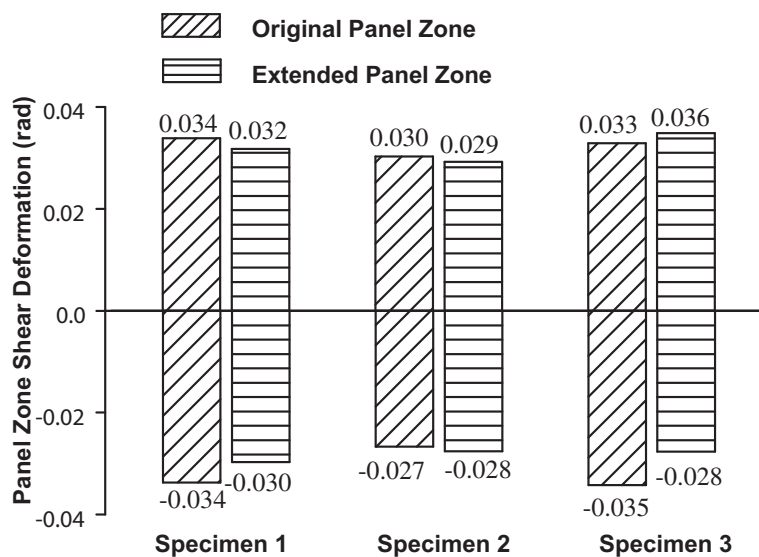


Fig. 11. Comparison of panel zone shear deformation.

Column-Flange Kinking and CJP Weld Fracture

Large panel zone deformation caused the column flange to kink at four corners of the panel zone. Figure 13 shows localized yielding of the flange on the backside of the column. On the front side, the location of the rehabilitated notch-tough CJP welded joint also coincided with one panel zone kinking location in specimens 2 and 3 (see Figure 9). Although these connections performed adequately to satisfy AISC 341-10 for special moment frames, repeated loading eventually caused fracture of the notch-tough CJP welds at the kinking locations. The relationship between CJP weld fracture and panel zone deformation is presented next.

WELD FRACTURE AND PANEL ZONE DEFORMATION CAPACITY

The panel zone behavior was extensively researched (e.g., Krawinkler, Bertero and Popov, 1971; Krawinkler, 1978; Kato, Chen and Nakao, 1988; Schneider and Amidi, 1998; El-Tawil et al., 1999; Lee et al., 2005). As will be shown, past research was mainly focused on the strength, not deformation capacity, of the panel zone, and the nominal shear strength of the panel zone in AISC 360 corresponds to a deformation at four times the yield shear strain. In this section, the relationship between CJP weld fracture and panel zone deformation is studied. Also, in performance-based

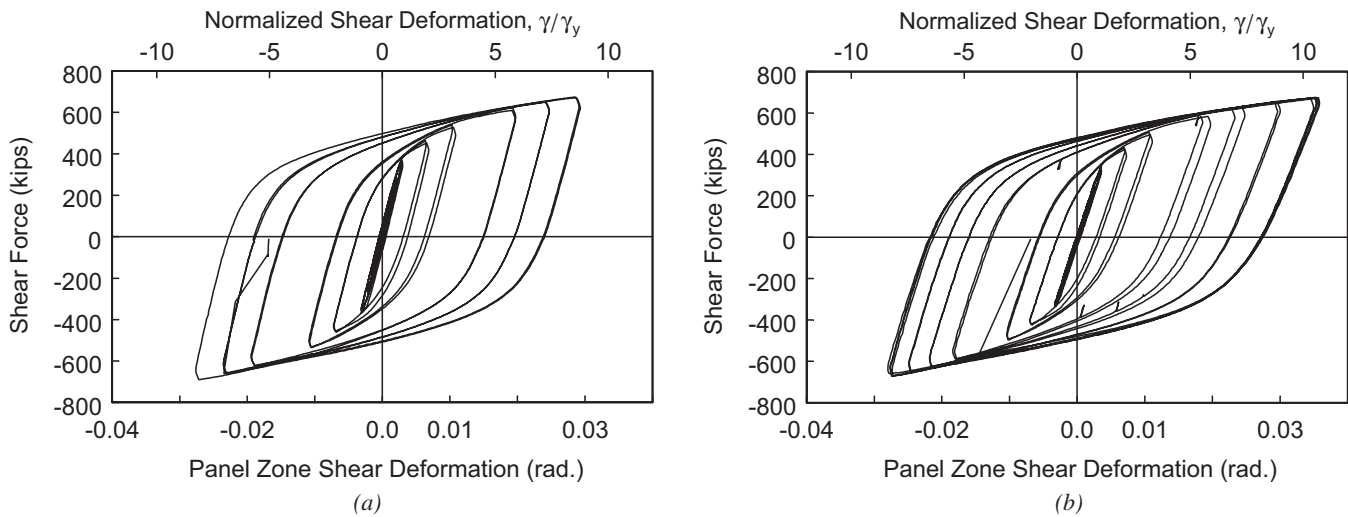


Fig. 12. Cyclic response of extended panel zone: (a) specimen 2; (b) specimen 3.

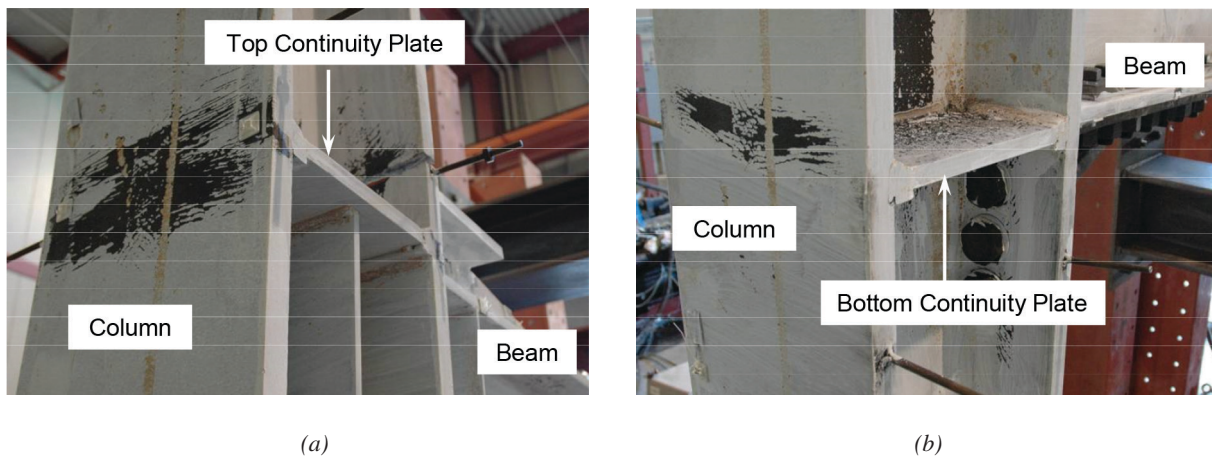


Fig. 13. Yielding pattern at column back side (specimen 3): (a) at top continuity plate level; (b) at bottom continuity plate level.

seismic analysis and design of tall buildings, PEER/ATC 72-1 (PEERC/ATC, 2010) suggested that a panel zone deformation capacity of 0.08 radian be used when panel zone shear distortion does not contribute to the incident of fractures at the beam-to-column connection. This deformation capacity is consistent with that accepted for link elements in eccentrically braced frames in AISC 341-10 (AISC, 2010b). Otherwise, a deformation capacity of 0.02 radian should be used when column-flange kinking would cause weld fracture at the beam-column connection. But no guidance is provided to determine when column-flange kinking is detrimental to weld fracture.

Krawinkler Model

Figure 14 shows the moment and shear diagrams of a column produced by seismic loading. The panel zone is in high shear with a reverse curvature (see Figure 15a). In the panel zone, the column web (together with doubler plates, if used) panel zone is bounded by two column flanges. Krawinkler (1978) used the superposition of column web and column flange in modeling the panel zone behavior. The column web was subjected to shear (see Figure 16a), where the web area was assumed to be $0.95d_c t_{cw}$, with d_c equal to the column depth and t_{cw} equal to the panel zone thickness and where the shear yield stress, τ_y , was $F_y/\sqrt{3}$ (equal to $0.577F_y$). The panel zone depth was also assumed to be $0.95d_b$, where d_b is the beam depth. A conservative assumption was made by ignoring strain hardening after yielding.

Although the bounding column flanges deform in reverse

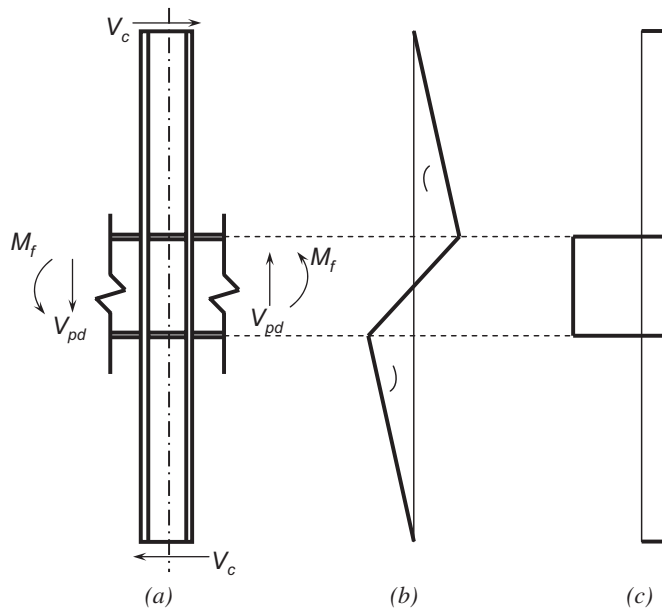


Fig. 14. Forces on column: (a) column free-body diagram; (b) moment diagram; (c) shear diagram.

curvature, Krawinkler modeled these flanges as rigid members and, instead, used rotational springs at four corners (i.e., kinking locations) of the panel zone to model the contribution from column flanges (see Figure 15b). It was assumed that column flanges contributed to both the stiffness and strength of the panel zone only when $\gamma \geq \gamma_y$, where $\gamma_y = \tau_y/G$ and G is the shear modulus. That is, the contribution from column flanges was ignored when $\gamma < \gamma_y$. Based on finite element analysis, Krawinkler et al. (1971) proposed the following rotational stiffness, K_s , at each corner:

$$K_s = \frac{M}{\theta} = \frac{Eb_{cf}t_{cf}^2}{10} \quad (4)$$

where b_{cf} is the column-flange width and t_{cf} is the column-flange thickness. Considering four rotational springs and the work equation $0.95d_b(\Delta V)(\Delta\gamma) = 4M\theta$ with $\theta = \Delta\gamma$, the proposed post-elastic stiffness, K_p , of the joint due to the column flanges (see Figure 16) was

$$K_p = \frac{\Delta V}{\Delta\gamma} = \frac{1.095b_{cf}t_{cf}^2G}{d_b} \quad (5)$$

Furthermore, the panel zone shear strength was defined at $4\gamma_y$. From the superposition shown in Figure 16, the following panel zone shear strength at $4\gamma_y$ was developed by Krawinkler (1978):

$$V_{pz}^K = 0.55F_y d_c t_{cw} \left(1 + \frac{3.45b_{cf}t_{cf}^2}{d_b d_c t_{cw}} \right) \quad (6)$$

AISC Design Strength

The AISC *Specification* (AISC, 2010c) uses $0.6F_y$ instead of $0.577F_y$ as τ_y . Furthermore, the web shear area is taken as $d_c t_{cw}$ instead of $0.95d_c t_{cw}$. The slightly modified form of Equation 6 is used in the AISC *Specification*:

$$V_{pz}^{AISC} = 0.6F_y d_c t_{cw} \left(1 + \frac{3b_{cf}t_{cf}^2}{d_b d_c t_{cw}} \right) \quad (7)$$

Alternate Panel Zone Model

It was shown in Figure 12 that a panel zone could deform to a deformation level much higher than $4\gamma_y$. But excessive deformation could cause fracture in the beam flange-to-column flange CJP weld. In this paper, an alternate model is presented to compute the ultimate deformation capacity and the associated strength of the panel zone. This deformation capacity uses the fracture of a notch-tough CJP weld at the column kinking location as the limit state. As will be

shown, the deformation capacity can be significantly higher than the $4\gamma_y$ value assumed in AISC 360-10. This model also shows that a panel zone's deformation can be less than $4\gamma_y$ in some situations.

The panel zone behavior is again established by superimposing the responses of the column web and flanges (see Figure 17). The web area is taken as $0.95d_c t_{cw}$. Therefore, the shear yield strength of the column web is

$$V_{cw,y} = 0.6F_y(0.95d_c t_{cw}) \quad (8)$$

With $\gamma_y = 0.6F_y/G$, the elastic shear stiffness of the column web is

$$K_{cw} = \frac{V_{cw,y}}{\gamma_y} = 0.95d_c t_{cw} G \quad (9)$$

The Krawinkler's model ignores strain hardening after yielding. But, because strain hardening generally exists for the steel grades ($F_y \leq 50$ ksi) permitted in AISC 341-10, a strain hardening ratio of 0.03 is adopted as shown in Figure 17a. The strain hardening ratio of 0.03 is based on

monotonic torsional coupon test results conducted by Slutter (1981).

Because each column flange in the panel zone region would bend about its weak axis in reverse curvature (see Figure 15a), the model in Figure 18a is used to consider the contribution from column flanges. It is idealized that each column flange will deform elastically until the plastic moment of the column flange is reached:

$$M_{p,cf} = \left(\frac{b_{cf} t_{cf}^2}{4} \right) F_{yc} \quad (10)$$

where F_{yc} is the column-flange yield stress. The associated deformation, which is the chord angle in Figure 18b, corresponds to γ_{pz} in Figure 17. It is postulated that γ_{pz} can be defined as the plastic deformation capacity of the panel zone beyond which the notch-tough CJP weld at the kinking locations is prone to fracture. This postulation is to be verified by test data in the following.

Consider one fix-ended column-flange flexural member with a span of $0.95d_b$ and a depth of t_{cf} . The shearing effect

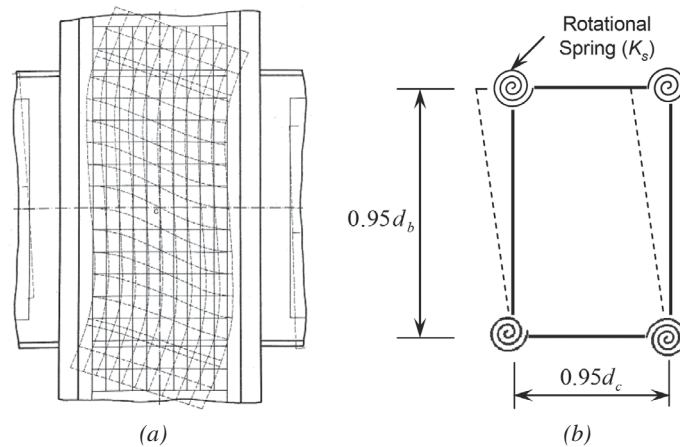


Fig. 15. Krawinkler's model of panel zone: (a) panel zone deformed shape; (b) mathematical model (figures reprinted from Krawinkler, 1978).

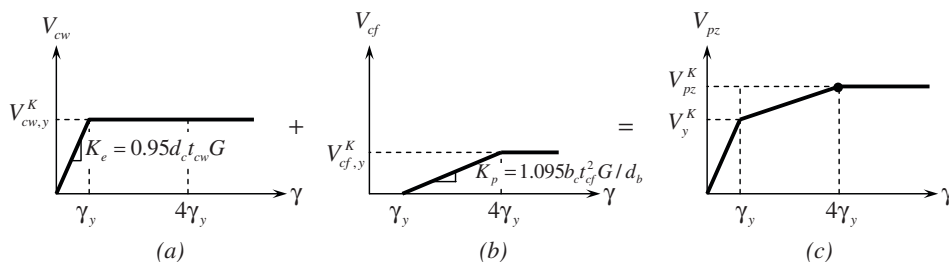


Fig. 16. Superposition of shear strength components per Krawinkler's model: (a) column web component; (b) column flange component; (c) superposition.

of this flexural member can be significant when the span is small (smaller d_b) and the column flange, t_{cf} , is thick. Applying elastic beam theory, the midspan deflection when the fixed-end moment reaches $M_{p,cf}$ is

$$\begin{aligned} \Delta &= \frac{1}{3EI_{cf}} \left[\frac{M_{p,cf}}{(0.95d_b/2)} \right] \left(\frac{0.95d_b}{2} \right)^3 \\ &+ \frac{1}{GA_{s,cf}} \left[\frac{M_{p,cf}}{(0.95d_b/2)} \right] \left(\frac{0.95d_b}{2} \right) \\ &= \left[\frac{d_b^2}{1.11t_{cf}^2} + 3.12 \right] \frac{M_{p,cf}}{Eb_{cf}t_{cf}} \\ &= \left[\frac{\alpha^2}{1.11} + 3.12 \right] \frac{M_{p,cf}}{Eb_{cf}t_{cf}} \end{aligned} \quad (11)$$

In Equation 11, the coefficient α is the span-depth ratio of the column-flange flexural member:

$$\alpha = d_b/t_{cf} \quad (12)$$

The first term on the right-hand side in Equation 11 is the flexural component, and the second term is the shearing component, where $I_{cf} = b_{cf}t_{cf}^3/12$ and $A_{s,cf} = 5b_{cf}t_{cf}/6$ are the moment of inertia and shear area of one column flange, respectively. Dividing Δ by $0.95d_b/2$ and simplifying gives the shear deformation capacity of the panel zone (see Figure 18):

$$\gamma_{pz} = \frac{0.475F_{yc}}{E} \left(\alpha + \frac{3.45}{\alpha} \right) \quad (13)$$

The elastic stiffness of one column flange is

$$K_{cf} = \frac{V_{p,cf}}{\gamma_{pz}} = \frac{2M_{p,cf}}{0.95d_b\gamma_{pz}} = \frac{1.11Eb_{cf}t_{cf}}{\alpha^2 + 3.45} \quad (14)$$

The total elastic stiffness for both column flanges is $2K_{cf}$, as shown in Figure 17b. Therefore, the total panel zone shear

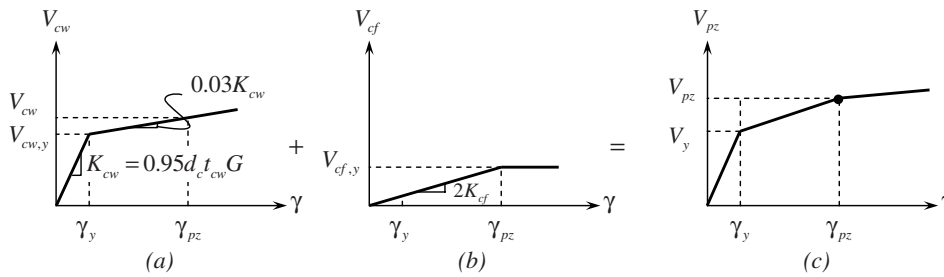


Fig. 17. Superposition of proposed shear strength components: (a) column web panel zone response; (b) response of two column flanges; (c) superposition.

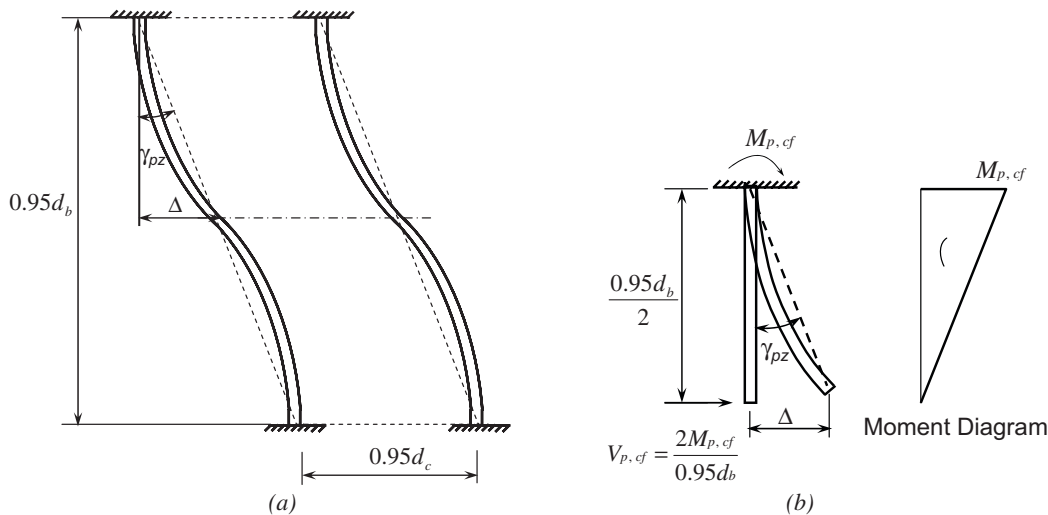


Fig. 18. Panel zone model: (a) panel zone deformation; (b) mathematical model.

strength in the elastic range is

$$V_{pz} = (K_{cw} + 2K_{cf})\gamma \text{ when } 0 \leq \gamma \leq \gamma_y \quad (15)$$

When $\gamma_y < \gamma \leq \gamma_{pz}$, the component of panel zone shear strength due to column web is (see Figure 17a)

$$V_{cw} = V_{cw,y} + 0.03K_{cw}(\gamma - \gamma_y) \quad (16)$$

The component of panel zone shear strength due to two column flanges is

$$V_{cf} = 2K_{cf}\gamma \quad (17)$$

Therefore, the total panel zone shear strength is

$$V_{pz} = V_{cw} + V_{cf} \text{ when } \gamma_y < \gamma \leq \gamma_{pz} \quad (18)$$

Based on Equations 15 and 18, and replacing d_b with d_{eff} , the predicted panel zone responses for specimens 2 and 3 up to γ_{pz} are shown in Figure 19. Specimen 1 was not used in this correlation because replacement CJP welds were not used and existing CJP weld locations did not coincide with the column kinking locations. The ratios between the predicted and experimental panel zone ultimate deformations are 1.02 and 0.94 for specimens 2 and 3, respectively.

Normalizing the panel zone deformation capacity, γ_{pz} , in Equation 13 by $\gamma_y = 0.6F_y/G$ gives the following:

$$\frac{\gamma_{pz}}{\gamma_y} = 0.30 \left(\alpha + \frac{3.45}{\alpha} \right) \quad (19)$$

Figure 20 shows the variation of the normalized panel zone shear deformation with respect to $\alpha = d_b/t_{cf}$. It is shown that the AISC assumed panel zone deformation capacity, $4\gamma_y$,

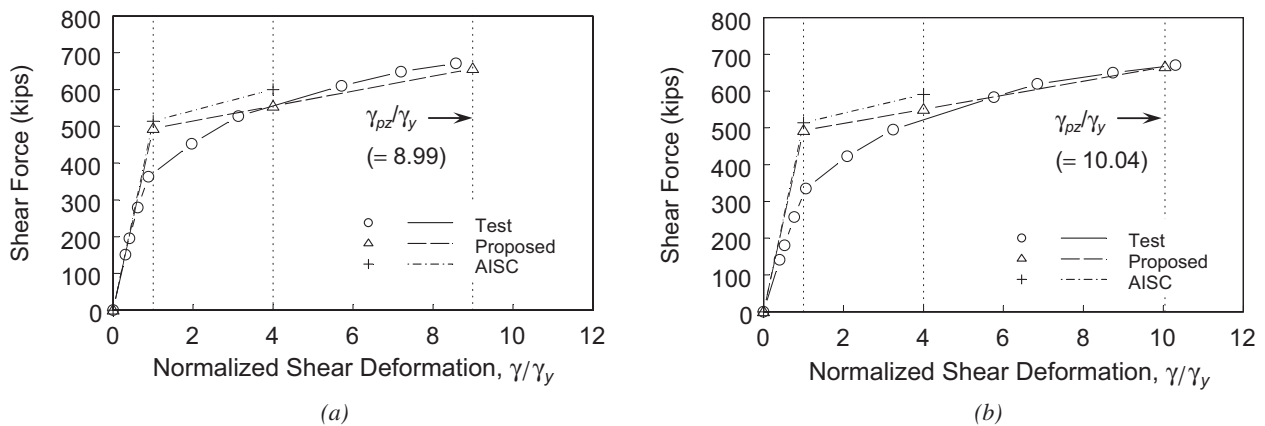


Fig. 19. Comparison of panel zone responses: (a) specimen 2; (b) specimen 3.

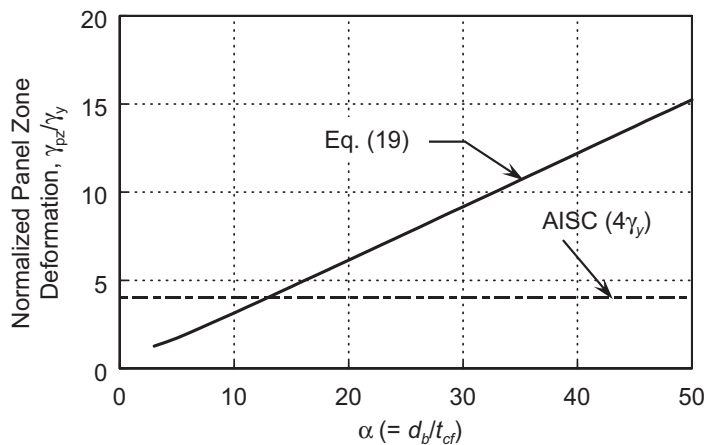


Fig. 20. Relationship between panel zone shear deformation and α .

can be very conservative for a high d_b/t_{cf} ratio. When the d_b/t_{cf} ratio is low (i.e., a shallow beam connected to a thick column flange), the panel zone deformation can be lower than $4\gamma_y$. Therefore, column flanges at kinking locations would yield early when d_b/t_{cf} is low, which makes the beam flange-to-column flange CJP welds more prone to fracture at a low panel zone deformation ($\leq 4\gamma_y$). This observation is valid for either rehabilitated or newly constructed moment connections.

Effect of Column Axial Force

With the presence of an axial load, Krawinkler et al. (1971) reported that column flanges carry all the axial load after the panel zone web has completely yielded. This is also the basis of the panel zone design shear strength with high axial load in AISC 360-10.

A column-flange cross-section and the stress distribution for the plastic moment condition are shown in Figure 21. The total stress distribution can be separated into the contributions of the axial force and bending moment. Because each column flange takes half of the column axial load, P , the axial stress equilibrium of one column flange is

$$\frac{P}{2} = (2y_p - t_{cf}) b_{cf} F_{yc} \quad (20)$$

The axial demand-capacity ratio of one column flange is

$$\frac{P/2}{P_{y,cf}} = \frac{(2y_p - t_{cf}) b_{cf} F_{yc}}{b_{cf} t_{cf} F_{yc}} = \frac{2y_p - t_{cf}}{t_{cf}} \quad (21)$$

where $P_{y,cf} = A_f F_{yc} = b_{cf} t_{cf} F_{yc}$ is the axial yield strength of one column flange and y_p designates the plastic neutral axis location. Therefore, the plastic neutral axis location is

$$y_p = \frac{t_{cf}}{2} \left(1 + \frac{P}{2P_{y,cf}} \right) \quad (22)$$

The reduced moment capacity of one column flange can be derived from Figure 21 as

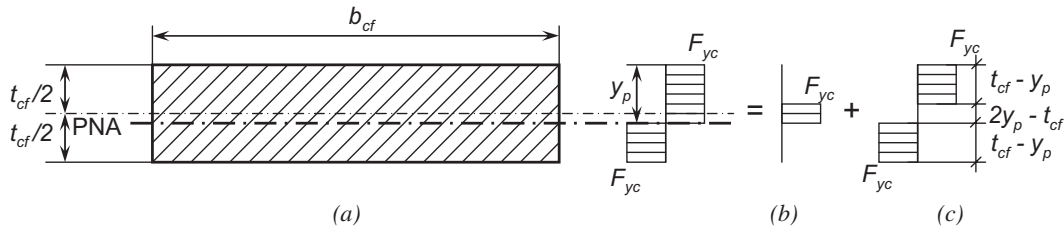


Fig. 21. Stress distribution of one column flange cross-section: (a) stress distribution in one column flange; (b) axial component; (c) flexural component.

$$\begin{aligned} M'_{p,cf} &= 2(t_{cf} - y_p) b_{cf} F_y \left(\frac{t_{cf}}{2} - \frac{t_{cf} - y_p}{2} \right) \\ &= M_{p,cf} \left[1 - \left(\frac{P}{2P_{y,cf}} \right)^2 \right] \end{aligned} \quad (23)$$

The corresponding shear of one column-flange flexural member in Figure 18 is

$$V'_{p,cf} = \frac{2M'_{p,cf}}{0.95d_b} = V_{p,cf} \left[1 - \left(\frac{P}{2P_{y,cf}} \right)^2 \right] \quad (24)$$

Following the similar procedure described in Equations 11 and 13, the reduced plastic shear deformation can be derived by replacing $M_{p,cf}$ and $V_{p,cf}$ with $M'_{p,cf}$ and $V'_{p,cf}$:

$$\begin{aligned} \gamma'_{pz} &= \frac{0.475F_{yc}}{E} \left(\alpha + \frac{3.45}{\alpha} \right) \left[1 - \left(\frac{P}{2P_{y,cf}} \right)^2 \right] \\ &= \gamma_{pz} \left[1 - \left(\frac{P}{2P_{y,cf}} \right)^2 \right] \end{aligned} \quad (25)$$

Figure 22 shows the effect of column axial load on the panel zone deformation capacity.

The associated panel zone shear strength at γ'_{pz} is established as follows. The component of panel zone shear strength due to column web from Equation 16 can be approximated as

$$V'_{cw} = V_{cw,y} + 0.03K_{cw} (\gamma'_{pz} - \gamma_y) \quad (26)$$

From Equation 24, the component of the panel zone shear strength due to two column flanges is

$$V'_{cf} = 2V'_{p,cf} = 2V_{p,cf} \left[1 - \left(\frac{P}{2P_{y,cf}} \right)^2 \right] \quad (27)$$

Therefore, the total panel zone shear strength is

$$V'_{pz} = V'_{cw} + V'_{cf} \quad (28)$$

Figure 23 shows example plots of the panel zone axial load–shear strength interaction curves. A W36×150 beam with three different W14 column sections in Figure 23a and W36 column sections in Figure 23b are considered. It is observed that axial load has a more significant effect on the panel zone deformation capacity than on the shear strength. Because the interaction between axial load and panel zone shear strength is relatively weak, the axial load effect can be ignored for simplicity when $P/2P_{y,cf} < 0.6$ (or $P/P_{y,cf} < 1.2$).

SUMMARY AND CONCLUSIONS

Three full-scale specimens were tested to evaluate the cyclic performance of rehabilitated pre-Northridge steel beam-to-column moment connections. The rehabilitation included

a Kaiser bolted bracket (KBB) on the beam bottom flange for all specimens, but different rehabilitation schemes were used to strengthen the beam top flange, which included the use of another KBB (specimen 1), a notch-tough complete-joint-penetration (CJP) beam flange replacement weld (specimen 2) or a welded double-tee bracket together with a replacement weld (specimen 3).

Test results showed that the proposed rehabilitation schemes adequately protected the existing pre-Northridge moment connections to the acceptable interstory drift angle. Large panel zone deformation with significant yielding occurred in all specimens; only specimen 1 also experienced beam buckling. Significant column kinking due to large panel zone deformation caused brittle fracture of the notch-tough CJP welds in specimens 2 and 3; panel zone deformation reached 0.029 rad and 0.036 rad in these specimens, respectively. Because these fractured welds were located at the column kinking locations, the test results provided useful information to verify the proposed panel zone

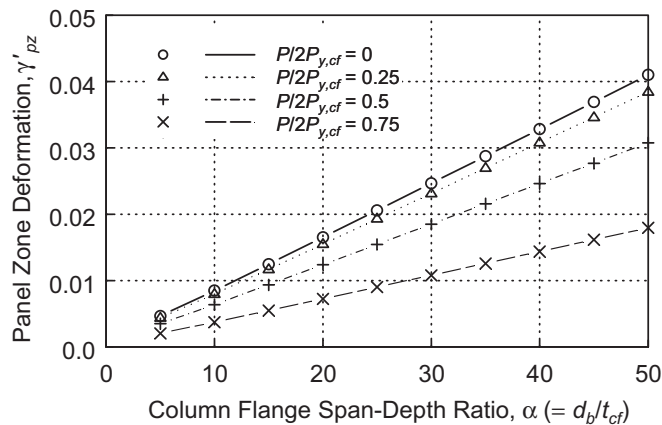


Fig. 22. Effect of column axial load on panel zone shear deformation capacity (ASTM A992 steel).

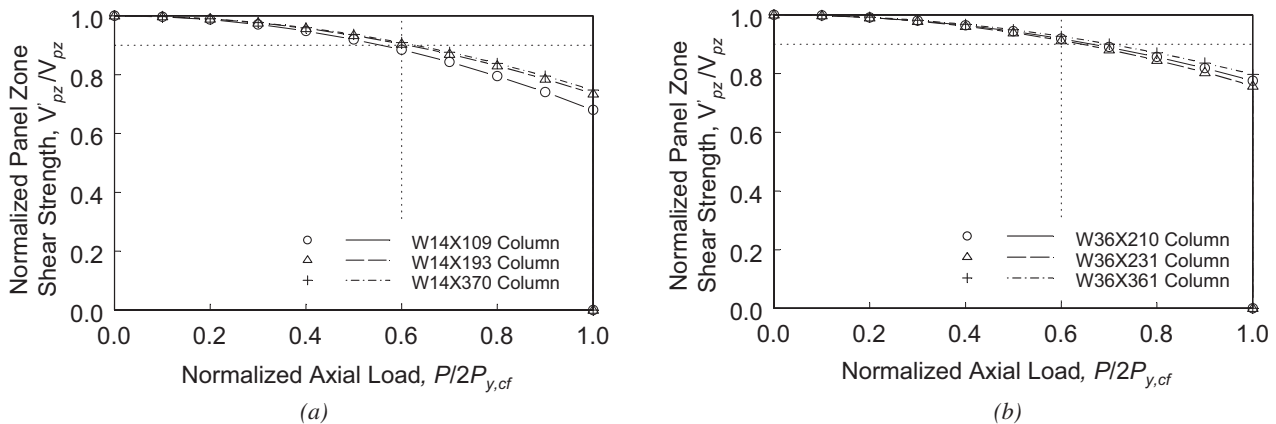


Fig. 23. Interaction of shear and axial force: (a) W14 columns; (b) W36 columns.

ultimate deformation capacity model, which used the fracture of notch-tough CJP welds at the kinking location as the limit state; the effect of column axial load was also included in the model formulation. The conclusions are summarized as follows.

1. The panel zone shear strength specified in AISC 360 corresponds to a shear deformation of $4\gamma_y$. But test results showed that the panel zone can deform more than $8\gamma_y$, although column kinking due to excessive panel zone deformation eventually caused weld fracture. Because it may not be economical and practical in seismic rehabilitation to avoid weak panel zones, a model (Figure 18) was proposed to predict the deformation capacity of the panel zone. It was postulated that the notch-tough beam flange CJP weld would fracture when the column flange was fully yielded at the kinking location. This limit state was used to define the ultimate deformation capacity of the panel zone. This postulation was calibrated with specimens 2 and 3, which experienced weld fracture. (For specimen 1, no CJP welds were located at the kinking locations.) The proposed model (see Equations 13 or 19) showed that the deformation capacity is a function of d_b/t_{cf} , where d_b = beam depth and t_{cf} = column flange thickness. The panel zone deformation capacity is small when the d_b/t_{cf} ratio is low (i.e., when a shallow beam is connected to a thick column flange), which results in earlier yielding of the column flanges at the kinking locations and makes the CJP welds more vulnerable to fracture.
2. The associated panel zone shear strength at the proposed deformation capacity level was also derived. In addition, the effect of column axial load on both the panel zone shear strength and deformation was also considered in the formulation. Its effect on the shear deformation capacity can be significant (see Equation 25). But the effect on shear strength is relatively insignificant (see Figure 23) and can be ignored when the column axial load is less than 1.2 times the yield force of one column flange.

The proposed model is also applicable to other moment connection types where the notch-tough CJP welds, not the pre-Northridge E70T-4 welds, are located at the column kinking locations. The test data available for calibrating the proposed model are scarce; only two specimens from this test program were available. Additional testing of moment connections that subject the panel zone to large deformation to induce beam flange weld fracture is needed to confirm the proposed model and to verify that the d_b/t_{cf} ratio is a key factor in determining the panel zone ultimate deformation.

ACKNOWLEDGMENTS

This project was sponsored by Civic Facilities Division of the City of Fremont and the City of Fremont Police Department. Crosby Group provided test specimen designs and technical guidance throughout the project. Steel Cast Connections provided the bolted bracket assemblies for all specimens.

REFERENCES

- Adan, S.M. and Gibb, W. (2009), "Experimental Evaluation of Kaiser Bolted Bracket Steel Moment Resisting Connections," *Engineering Journal*, AISC, Vol. 46, No. 3, pp. 181–193.
- AISC (2010a), *Prequalified Connections for Special and Intermediate Steel Moment Frames for Seismic Applications*, ANSI/AISC 358-10, American Institute of Steel Construction, Chicago, IL.
- AISC (2010b), *Seismic Provisions for Structural Steel Buildings*, ANSI/AISC 341-10, American Institute of Steel Construction, Chicago, IL.
- AISC (2010c), *Specification for Structural Steel Buildings*, ANSI/AISC 360-10, American Institute of Steel Construction, Chicago, IL.
- Blaney, C., Uang, C.M., Kim, D.W., Sim, H.B. and Adan, S.M. (2010), "Cyclic Testing and Analysis of Retrofitted Pre-Northridge Steel Moment Connections Using Bolted Brackets," *Proceedings*, Annual Convention, Structural Engineers Association of California, Sacramento, CA.
- El-Tawil, S., Vidarsson E., Mikesell T. and Kunnath, S.K. (1999), "Inelastic Behavior and Design of Steel Panel Zones," *Journal of the Structural Division*, ASCE, Vol. 125, No. 2, pp. 183–193.
- Gross, J.L., Engelhardt, M.D., Uang, C.M., Kasai, K. and Iwankiw, N.R. (1999), "Modification of Existing Welded Steel Moment Frame Connections for Seismic Resistance," *AISC Design Guide No. 12*, American Institute of Steel Construction, Chicago, IL.
- Kasai, K., Hodgson, I. and Bleiman, D. (1998), "Rigid-Bolted Repair Methods for Damaged Moment Connections," *Engineering Structures*, Vol. 20, No. 4–6, pp. 521–532.
- Kato, B., Chen, W.F. and Nakao, M. (1998), "Effects of Joint-Panel Shear Deformation on Frames," *Journal of Constructional Steel Research*, Vol. 10, pp. 269–320.
- Krawinkler, H., Bertero, V.V. and Popov, E.P. (1971), "Inelastic Behavior of Steel Beam-to-Column Subassemblages," EERC Report No. 71-7, University of California, Berkeley, CA.
- Krawinkler, H. (1978), "Shear in Beam-Column Joints in Seismic Design of Steel Frames," *Engineering Journal*, AISC, Vol. 5, No. 3, pp. 82–91.

- Lee, D., Cotton, S.C., Hajjar, J.F., Dexter, R.J. and Ye, Y. (2005), "Cyclic Behavior of Steel Moment-Resisting Connections Reinforced by Alternative Column Stiffener Details II. Panel Zone Behavior and Doubler Plate Detailing," *Engineering Journal*, AISC, Vol. 42, No. 4, pp. 215–238.
- Liu, W., Givens, D., Kantikar, R. and Blaney, C. (2009), "Seismic Evaluation and Rehabilitation of a Three Story Pre-Northridge Steel Frame Essential Service Facility," *Proceedings*, ATC & SEI Conference on Improving the Seismic Performance of Buildings and Other Structures, pp. 56–67, American Society of Civil Engineers, Reston, VA.
- Newell, J. and Uang, C.M. (2006), "Cyclic Testing of Steel Moment Connections for the CALTRANS District 4 Office Building Seismic Rehabilitation," UCSD Report No. SSRP-05/03, Department of Structural Engineering, University of California, San Diego, CA.
- PEERC/ATC (2010), *Modeling and Acceptance Criteria for Seismic Design and Analysis of Tall Buildings*, PEER/ATC 72-1, Pacific Earthquake Engineering Research Center and Applied Technology Council.
- Schneider, S.P. and Amidi, A. (1998), "Seismic Behavior of Steel Frames with Deformable Panel Zones," *Journal of the Structural Division*, ASCE, Vol. 124, No. 1, pp. 35–42.
- Slutter, R.G. (1981), "Test of Panel Zone Behavior in Beam-Column Connections," Report No. 200.81.403.1, Fritz Engineering Laboratory, Lehigh University, Bethlehem, PA.